Journal of Alloys and Compounds 509 (2011) 8028–8031

Contents lists available at ScienceDirect

Journal of Alloys and Compounds

journal homepage: www.elsevier.com/locate/jallcom

Effect of V doping on phase composition and electrical properties of $K_{0.4}Na_{0.6}Nb_{1-x}V_xO_3$ thin films

N. Li[a], W.L. Li[a,*], L.D. Wang[a], S.Q. Zhang[a], J.W. Ye[b], W.D. Fei[a]

[a] *Department of Materials Physics and Chemistry, Harbin Institute of Technology, Harbin 150001, PR China*
[b] *School of electronics engineering and computer science, Peking University, Peking 100871, PR China*

ARTICLE INFO

Article history:
Received 12 January 2011
Received in revised form 30 April 2011
Accepted 2 May 2011
Available online 24 May 2011

Keywords:
V doping
Phase composition
Electrical properties
Thin films

ABSTRACT

Lead-free $K_{0.4}Na_{0.6}Nb_{1-x}V_xO_3$ thin films were prepared by chemical solution deposition method. The effects of V doping on the phase composition and electrical properties of the films were studied at room temperature. The results indicate that the films are composed of orthorhombic and tetragonal phases, and the phase composition is affected by V content. It is also found that the ferroelectric and dielectric properties are improved by V doping ($2P_{r\max} = 35.5\ \mu C/cm$, $\varepsilon_{\max} = 1189$). The enhanced electrical properties are attributed to the more T-phase content and better quality of $K_{0.4}Na_{0.6}Nb_{1-x}V_xO_3$ ($x = 0.015$) film.

1. Introduction

Potassium sodium niobate ($K_xNa_{1-x}NbO_3$, KNN)-based ferroelectrics with ABO_3 perovskite structure, as one of the promising candidates for lead-based materials, have attracted much attention because of their good piezoelectric properties [1–3]. It has been reported that the piezoelectric properties of perovskite ferroelectrics are closely related to the morphotropic phase boundary (MPB) [4,5]. Furthermore, the MPB can affect the ferroelectric and piezoelectric properties of KNN-based ceramics [6,7]. Some recent studies [8,9] have shown that the coexistence of orthorhombic (O) and tetragonal (T) phases is helpful to obtain enhanced electrical properties of KNN-based ceramics, and the polymorphic phase transition (PPT) near room temperature is important for the composition design of KNN-based ceramics [10,11]. But the related studies about the phase coexistence in KNN-based films have been rarely reported.

The partial substitutions of A-site ions (Na^+ or K^+ for KNN) and B-site ion (Nb^{5+} for KNN) by other analogous ions in the ABO_3-type perovskite structure have been widely employed to improve the properties of ABO_3 ferroelectrics [12–14]. In previous studies, Sb^{5+}, Li^+, and Ta^{5+} have been used as the doping ions for the A-site or the B-site ions in KNN-based materials [15,16]. However, little work is done on the study of V doping. In addition, the poor quality of KNN films has not been thoroughly solved yet [17].

In the present letter, the effect of V doping on the microstructure, phase composition and electrical properties of KNN films has been studied. The atomic ratio of K/Na was selected as 40/60 in the study in view of the excellent properties of $K_{0.4}Na_{0.6}NbO_3$ ceramics [18–20]. The results provided in this paper clearly reveal that V doping is very effective to improve the quality and electrical properties of KNN films.

2. Experimental details

The thin films with the compositions of $K_{0.4}Na_{0.6}Nb_{1-x}V_xO_3$ (KNNV$_x$, $x = 0$, 0.005, 0.010, 0.015, 0.020) were prepared by chemical solution deposition. The precursors were prepared by mixing potassium acetate, sodium acetate, niobium ethoxide and vanadyl acetylacetonate in 2-methoxyethanol solvent, and the final precursor concentration was adjusted to 0.20 mol/L. The precursor of Nb_2O_5 with the concentration of 0.04 mol/L used as the seed layer was prepared by mixing the niobium ethoxide into 2-methoxyethanol solvent. The Nb_2O_5 precursor was firstly spin-coated on the (1 0 0) orientation Pt/Ti/SiO_2/Si substrates, and followed by pyrolysis at 375 °C for 10 min. The thickness of Nb_2O_5 seed layer is about 5 nm. Subsequently, the wet KNNV$_x$ films were spin-coated at 4000 rpm for 10 s on the Nb_2O_5 seed layer. Each layer was pyrolyzed at 375 °C for 10 min, and then the films were annealed at 675 °C for 5 min on a rapid thermal annealing (RTA) furnace in O_2 ambient. The thickness of the films used was about 350 nm.

X-ray diffraction (XRD) characterizations of the KNNV$_x$ thin films were performed on a philips X'pert diffractometer using Cu Kα radiation. The film surface and cross-sectional morphologies were observed by a FEI QUANTA 200F scanning electron microscope (SEM). The ferroelectric loops were evaluated on a Radiant Precision Workstation Ferroelectric Measurement System. The room temperature dielectric constants were measured on an Agilent 4294A analyzer.

3. Results and discussion

Fig. 1 shows the XRD patterns of KNNV$_x$ films with different V contents. The peaks are indexed by pseudo-cubic coordinates

---

[*] Corresponding author. fax: +86 451 86418647.
E-mail address: wlli@hit.edu.cn (W.L. Li).

0925-8388/$ – see front matter. Crown Copyright © 2011 Published by Elsevier B.V. All rights reserved.
doi:10.1016/j.jallcom.2011.05.002

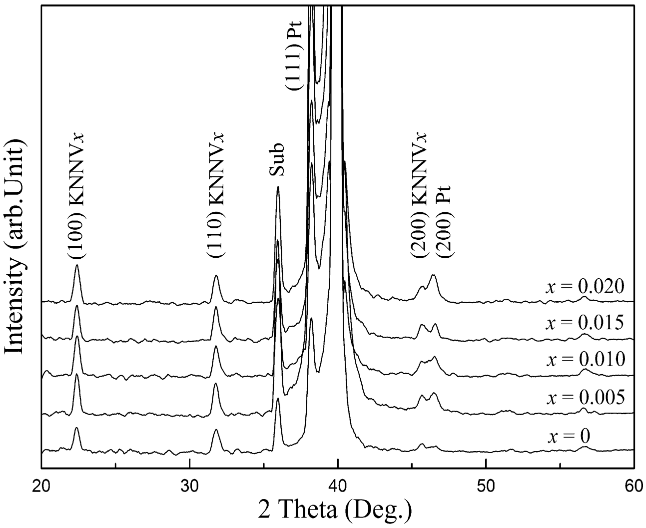

Fig. 1. XRD patterns of KNNV$_x$ films with different V contents.

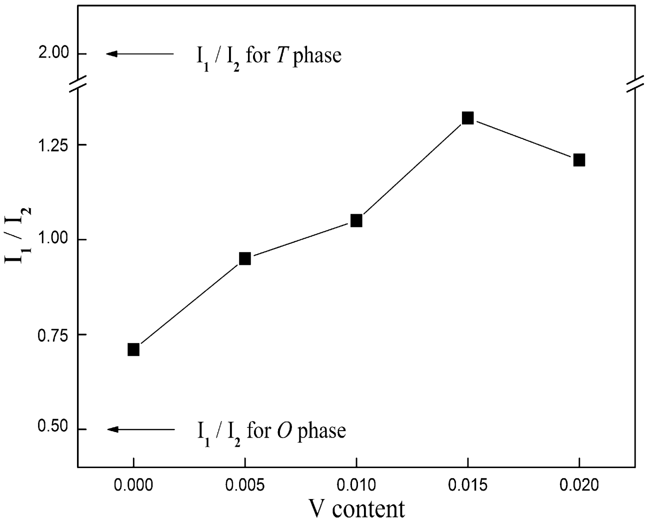

Fig. 3. Intensity ratio of the two separated peaks in the range of 2θ from 31.0° to 32.5°.

[21]. It is clear that the pure perovskite structure is obtained in the films, which indicates that V^{5+} seems to have diffused into the perovskite ABO_3 lattice. Because the V^{5+} and Nb^{5+} have the similar radius, and Nb^{5+} occupies the B-site, therefore, the V^{5+} will occupy the B-site of the ABO_3 structure as well. The fine scan XRD patterns and peak separations are shown in Fig. 2. The peaks for all the films can be divided into two separate peaks, namely, peak 1 at about 31.7° and peak 2 at about 31.9°. Because the lattice structure and lattice parameters of O- and T-phases are very similar, thereby peak 1 can be indexed as $(1\,1\,0)_O$ or $(1\,0\,1)_T$, and peak 2 can be indexed as $(1\,0\,1)_O$ or $(1\,1\,0)_T$ (the subscripts present O- or T-phase).

Fig. 3 gives the calculated intensity ratio of the two separated peaks in the range of 2θ from 31.0° to 32.5°. According to the multiplicity factors of diffraction peaks for O- and T-phases, the following results can be concluded: For pure O-phase of KNN films, the lattice parameters $a = c > b$ [6,19,22]. Based on the crystal symmetry of O-phase, the $(1\,1\,0)_O$ reflection is composed of $(1\,0\,1)$, $(\bar{1}\,0\,1)$, $(\bar{1}\,0\,\bar{1})$, and $(1\,0\,\bar{1})$, the $(1\,0\,1)_O$ reflection is composed of $(1\,1\,0)$, $(1\,\bar{1}\,0)$, $(\bar{1}\,\bar{1}\,0)$, $(\bar{1}\,1\,0)$, $(0\,1\,1)$, $(0\,\bar{1}\,1)$, $(0\,\bar{1}\,\bar{1})$, $(0\,1\,\bar{1})$, namely, the multiplicity factors of $(1\,0\,1)_O$ reflection is twice as many as that of $(1\,1\,0)_O$ reflection. Therefore, the intensity ratio of $I110_O/I101_O$ should be 0.5. According to the similar discussion, we can obtain that the intensity ratio of $I101_T/I110_T$ is 2.0 because $a = b < c$ for T-phase [6,19,22]. However, the intensity ratios of I_1/I_2 of the two peaks for all the KNNV$_x$ films are between 0.71 and 1.32, as shown in Fig. 3. In this regard, the abnormal intensity ratio of I_1/I_2 indicates that both O- and T-phases coexist in all the films. Moreover, the increasing intensity ratio of I_1/I_2 implies the increasing of T-phase content. As revealed in Fig. 3, T-phase content increases initially with V doping content increasing, and achieves its maximum value in KNNV$_{0.015}$ film. In contrast, as x value is more than 0.015, T-phase content decreases. The anomaly existing in Fig. 3 can probably be accounted for by the following two reasons. On the one hand, since the radius of V^{5+} (0.59 Å) is smaller than that of Nb^{5+} (0.69 Å), V partial substitution can cause the variation of the B-site ionic radius, leading to the lattice distortion referred to as the so-called 'chemical pressure' [23]. On the other hand, V doping changes the lattice constants, leading to the alteration of the film stress.

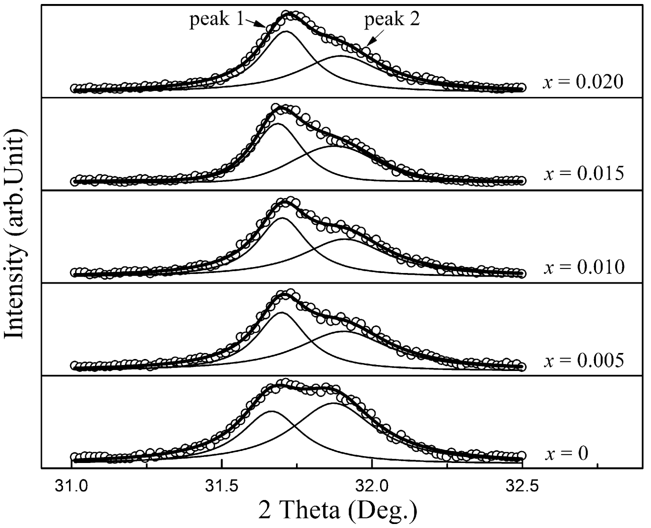

Fig. 2. Fine scan XRD patterns and peak separation in the range of 2θ from 31.0° to 32.5°.

The surface and cross-sectional morphologies of the KNNV$_x$ films are presented in Fig. 4. The similar cross-sectional micrographs can be found for the KNNV$_0$ and KNNV$_{0.015}$ films, as show in Fig. 4(b) and (d). However, the surface morphology of KNNV$_0$ film is quite different from that of KNNV$_{0.015}$ film. The grain size of KNNV$_0$ film is much larger than that of KNNV$_{0.015}$ film, and some micro-pores and micro-cracks (marked with arrows) in Fig. 4(a) are clearly visible in the grain boundaries of KNNV$_0$ film, but it is not the case in KNNV$_{0.015}$ film (Fig. 4(c)). The above results and analysis demonstrate that V doping is an effective approach to reduce the grain size and improve the quality of KNN films.

P–E hysteresis loops of the KNNV$_x$ films with different V contents were measured at room temperature, as shown in Fig. 5(a). It has been reported that the KNN film without seed layer is unable to get well hysteresis loop even at low electric field. By adding Nb_2O_5 seed layer to KNN films, the binding between the films and the substrates can be enhanced, leading to the reduction of leakage current of the films, so the well hysteresis loop can be gain [24]. In Fig. 5(a), it can be found that all the KNNV$_x$ films with Nb_2O_5 seed layer exhibit well saturated hysteresis loops. The KNN films with V doping show the well hysteresis loops under an electric field of about 500 kV/cm. However, the *P–E* hysteresis loop of KNNV$_0$ film fails to be measured at this

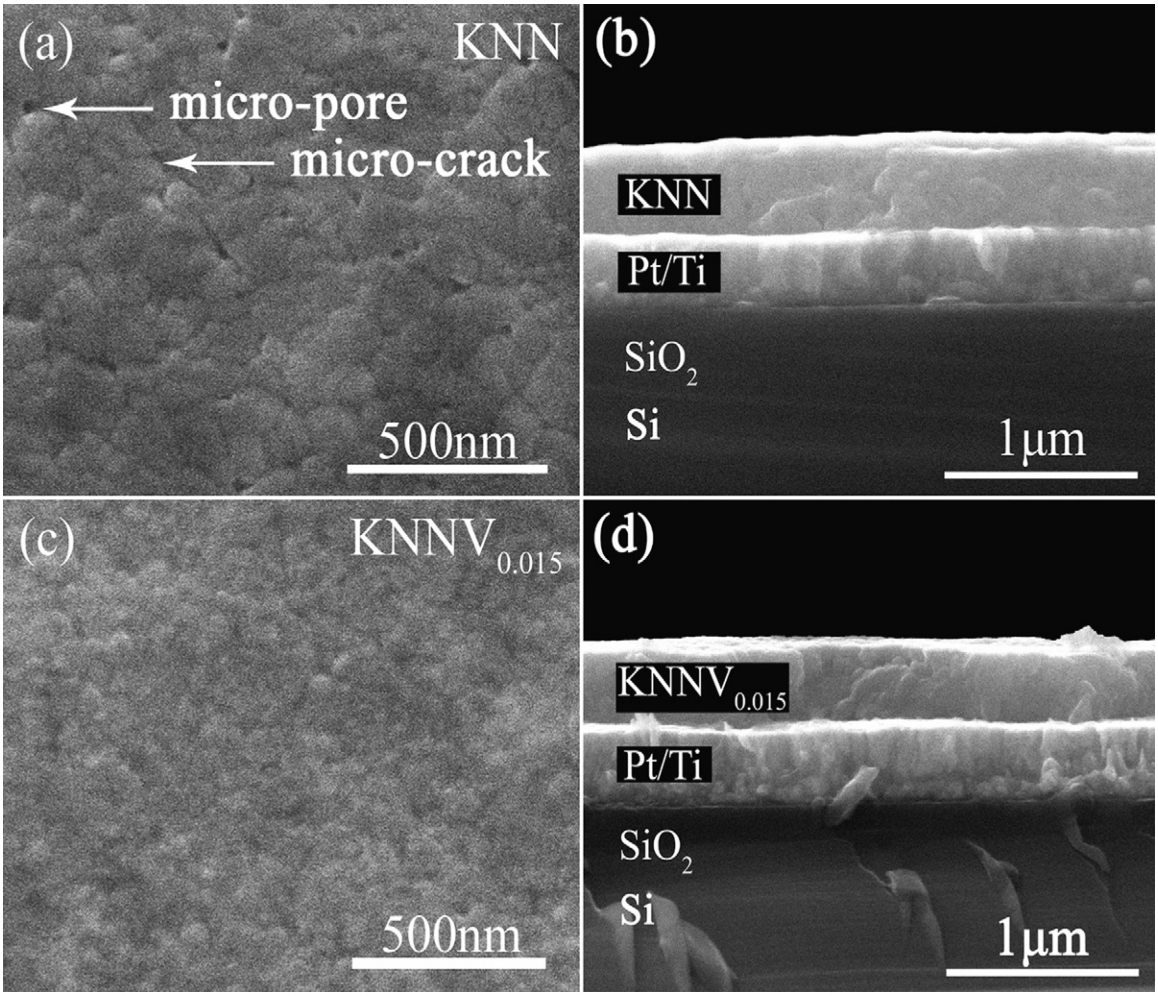

Fig. 4. SEM micrographs of $KNNV_0$ and $KNNV_{0.015}$ thin film (a) and (c) surface view and (b) and (d) cross-sectional view.

field. Fig. 5(b) displays the remnant polarization value ($2P_r$) for $KNNV_x$ films with different V contents. It can be seen that $2P_r$ value increases with the V content increasing, and attains the maximum value (35.5 μC/cm) at $x = 0.015$, and then decreases at $x = 0.020$.

Fig. 6 shows the relationship between dielectric constant at 1000 Hz for $KNNV_x$ films and different V contents at room temperature. The dielectric properties were measured under a signal voltage of 500 mV, and in the frequency range from 100 Hz to 2000 Hz. The dielectric constant increases with the V content

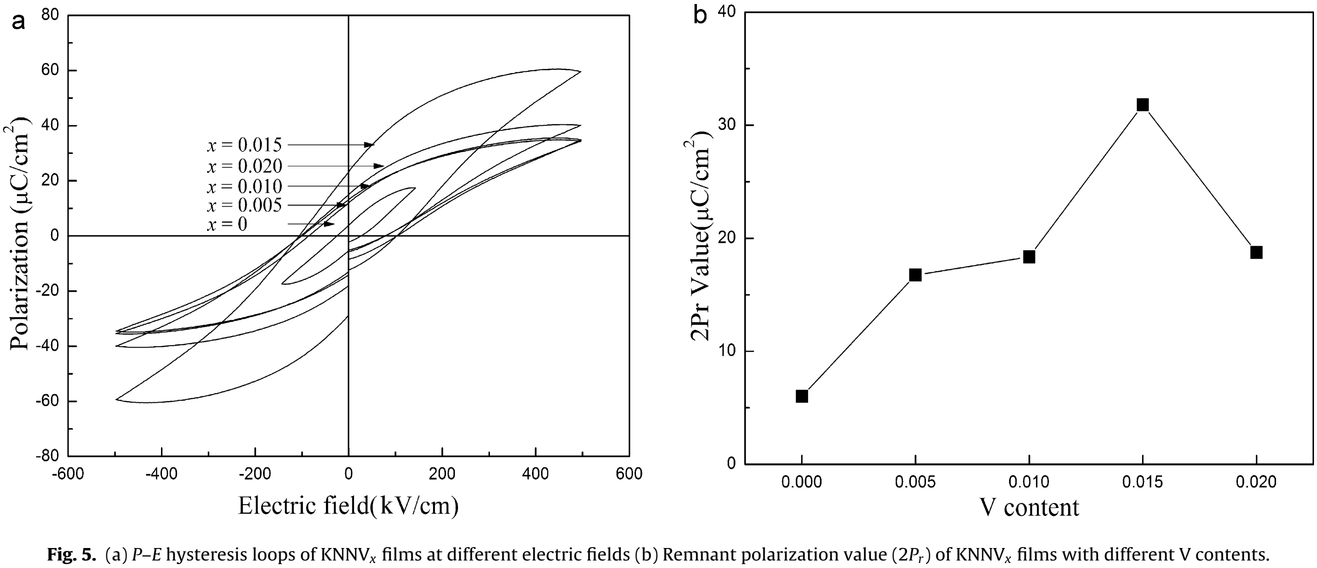

Fig. 5. (a) *P–E* hysteresis loops of $KNNV_x$ films at different electric fields (b) Remnant polarization value ($2P_r$) of $KNNV_x$ films with different V contents.

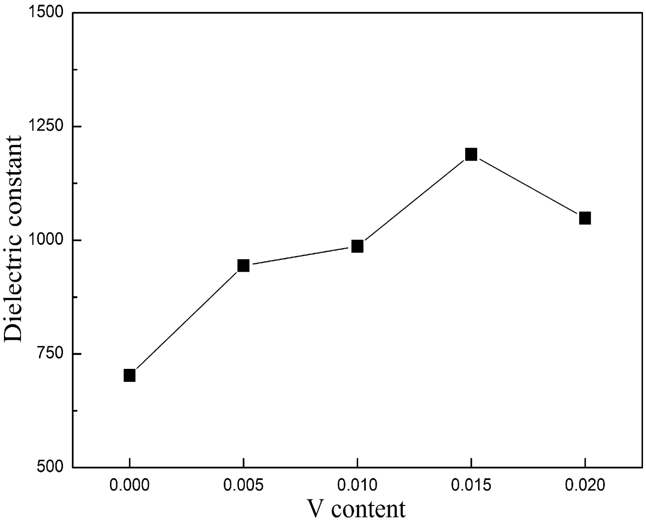

Fig. 6. Dielectric constant at 1 kHz of KNNV$_x$ films with different V contents.

increasing, and the KNNV$_{0.015}$ film gains the maximum value of dielectric constant ($\varepsilon = 1189$). The above results suggest that the KNNV$_{0.015}$ film may be near the O- and T-phases boundary [25].

4. Conclusions

In conclusion, proper V doping is an effective method to improve the quality of the KNN films, and enhance the ferroelectric and dielectric properties. By means of V doping, fine grains can be obtained, and the micro-pores and micro-cracks in the films can be healed. In addition, the films are composed of T-phase and O-phase due to the lattice distortion and stress effect in the films, and proper V doping can increase T-phase content. KNNV$_{0.015}$ film gains the best ferroelectric and dielectric properties in our study ($2P_r = 35.5\ \mu$C/cm, $\varepsilon = 1189$). These results illustrate that the $K_{0.4}Na_{0.6}Nb_{1-x}V_xO_3$ ($x = 0.015$) film is a promising electrical material for lead-free applications.

Acknowledgements

The project was supported by the Fundamental Research Funds for the Central Universities (grant no. HIT.KLOF.2010002); China Postdoctoral Science Foundation; Postdoctoral Fund of Heilongjiang Province. Thanks are given for M.H. Ding for his valuable help on XRD measurements and analysis.

References

[1] Y. Saito, H. Takao, T. Tani, T. Nonoyama, K. Takatori, T. Homma, T. Nagaya, M. Nakamura, Nature 432 (2004) 84–87.
[2] G. Shirane, R. Newnham, R. Pepinsky, Phys. Rev. B 96 (1954) 581–588.
[3] G.H. Haertling, J. Am. Ceram. Soc. 50 (1967) 329–330.
[4] B. Noheda, D.E. Cox, G. Shirane, R. Guo, B. Jones, L.E. Cross, Phys. Rev. B 63 (2000) 014103.
[5] B. Noheda, D.E. Cox, G. Shirane, J. Gao, Z.G. Ye, Phys. Rev. B 66 (2002) 054104.
[6] J.G. Wu, D.Q. Xiao, Y.Y. Wang, J.G. Zhu, P. Yu, Y.H. Jiang, J. Appl. Phys. 102 (2007) 114113.
[7] P. Zhao, B.P. Zhang, J.F. Li, Appl. Phys. Lett. 91 (2007) 172901.
[8] S.J. Zhang, R. Xia, T.R. Shrout, G.Z. Zang, J.F. Wang, J. Appl. Phys. 100 (2006) 104108.
[9] S.J. Zhang, R. Xia, T.R. Shrout, Appl. Phys. Lett. 91 (2007) 132913.
[10] E.K. Akdogan, K. Kerman, M. Abazari, A. Safari, Appl. Phys. Lett. 92 (2008) 112908.
[11] C. Lei, Z.G. Ye, Appl. Phys. Lett. 93 (2008) 042901.
[12] H. Birol, D. Damjanoric, N.J. Setter, Eur. Ceram. Soc. 26 (2006) 861–866.
[13] B. Malic, J. Bernard, J. Holc, D. Jenko, M.J. Kosec, Eur. Ceram. Soc. 25 (2005) 2707–2711.
[14] Y.P. Guo, K. Kakimoto, H. Ohsato, Solid State Commun. 129 (2004) 279–284.
[15] X.K. Niu, J.L. Zhang, L. Wu, P. Zheng, M.L. Zhao, C.L. Wang, Solid State Commun. 146 (2008) 395–398.
[16] Y.F. Chang, Z.P. Yang, D.F. Ma, Z.H. Liu, Z.L. Wang, J. Appl. Phys. 104 (2008) 024109.
[17] L.Y. Wang, K. Yao, W. Ren, Appl. Phys. Lett. 93 (2008) 092903.
[18] Z.P. Yang, Y.F. Chang, W.L. Li, Appl. Phys. Lett. 90 (2007) 042911.
[19] J.G. Wu, D.Q. Xiao, Y.Y. Wang, J.G. Zhu, L. Wu, Y.H. Jiang, Appl. Phys. Lett. 91 (2007) 252907.
[20] J.G. Wu, D.Q. Xiao, Y.Y. Wang, J.G. Zhu, P.J. Yu, Appl. Phys. Lett. 103 (2008) 024102.
[21] C.Q. Liu, W.L. Li, W.D. Fei, S.Q. Zhang, J.N. Wang, J. Alloys Compd. 493 (2010) 499–501.
[22] J.G. Hao, R.Q. Chu, Z.J. Xu, G.Z. Zang, G.R. Li, J. Alloys Compd. 479 (2009) 376–380.
[23] M. Ahart, M. Somayazulu, R.E. Cohen, P. Ganesh, P. Dera, H.K. Mao, R.J. Hemley, Y. Ren, P. Liermann, Z.G. Wu, Nature 451 (2008) 545–552.
[24] N. Li, W.L. Li, L.D. Wang, S.Q. Zhang, W.D. Fei, Mater. Lett. 65 (2011) 1010–1013.
[25] J.R. Cheng, W.Y. Zhu, N. Li, L.E. Cross, J. Appl. Phys. 91 (2002) 5997–6001.